Index

Paper 6.4

Investigation of the Installation Effects on Ultrasonic Flowmeters and Evaluation of Computational Fluid Dynamics Prediction Methods

Craig J. Coull, NEL
Neil A. Barton, NEL

Investigation of the Installation Effect on Ultrasonic Flowmeters and Evaluation of Computational Fluid Dynamics Prediction Methods

Craig J. Coull, NEL
Neil A, Barton, NEL

SUMMARY

This paper presents the results of a detailed investigation of installation effects on the performance of transit time ultrasonic flow meters. Extensive laboratory tests and Computational Fluid Dynamics (CFD) modelling have been performed.

Laboratory tests have been carried out on a triple bend installation. Three meters have been tested two clamp-on meters (reflect diametric paths) and a dual-cross mid-radius meter.

Each meters performance has been analysed and explanations offered as to why the observed effects occur. Path velocity data has also been recorded from the dual-cross mid-radius meter. This data has been used to reconstruct other mid-radius meter designs and allow their performance to be analysed. Also the diagnostic capabilities of individual path velocities in mid-radius design meters have been considered.

The final section of the paper presents the results of the CFD modelling of the laboratory experiments. These results are analysed using the laboratory results including a pitot tube traverse of the test section.

BACKGROUND

Ultrasonic flowmeters are increasingly being used for fiscal metering purposes in the oil and gas industry. As they are relatively new to the market and there are many different designs, the influence of upstream bends and fittings on the performance of ultrasonic meters has not been well characterised. The number of tests required to determine the performance of all of the common ultrasonic meter designs to all of the potential installations in which they may be used is prohibitive. One potential solution is to use Computational Fluid Dynamics (CFD) flow modelling techniques to study ultrasonic flowmeters in non-standard installations and in doing so, reduce the number of tests needed to determine the uncertainty of a particular flowmeter in a particular installation.

The use of CFD as an aid to understanding the uncertainty of ultrasonic flowmeters installed downstream of different fittings was studied in one of the projects in the 1996-99 Flow Programme (Reference 1). This work showed that CFD predictions match test measurements well, as illustrated in Figure 1. In particular, good matches were achieved downstream of a contraction and a twisted double bend. However, installation errors were over-estimated in dual diametric meters immediately downstream of an expansion and in a dual diametric meter immediately downstream of a single bend.

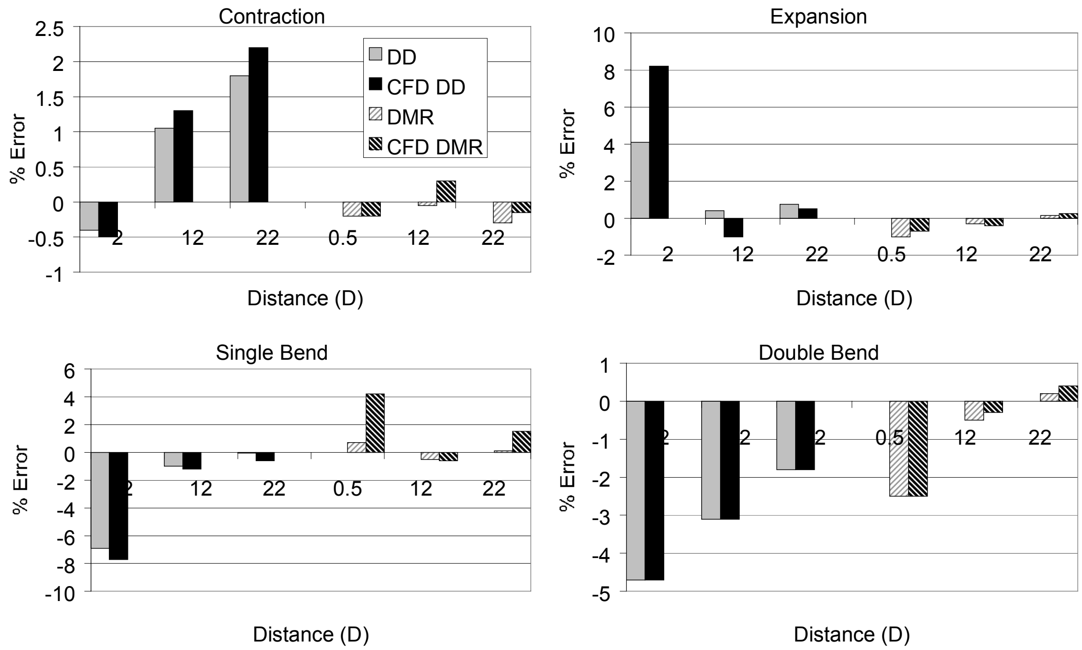

Figure 1. Comparison of measured and predicted installation error of dual diametric (DD) and dual mid-radius (DMR) ultrasonic flowmeters downstream of different pipework fittings

This paper discusses follow-on work performed as part of the 1999-2002 Flow Programme in which the installation effect downstream of a triple bend installation is studied. In this work more detailed measurements and further simulations have been taken to ascertain the cause and severity of the effect and to determine how different meter designs respond to this type of flow disturbance. This work has important implications for the design of fiscal metering stations using ultrasonic meters.

INTRODUCTION

This paper discuses the laboratory work performed as part of the 1999-2002 Flow Programme Project “In-Service Performance of Ultrasonic Flow Meters”. This project has investigated installation effects as these have been identified as having a major effect on in-service performance. In conjunction with the laboratory tests, CFD modelling has been performed and the results compared to evaluate the modelling technique’s ability to predict installation effect.

A case study on a single installation was considered most appropriate, as this would allow extensive experimental testing to be carried out. The triple bend was chosen since it was considered reasonably representative, as any single installation can be, of pipework upstream of a metering installation.

METER TYPES

Three meters were supplied to NEL for the project “In-Service Performance of Ultrasonic flowmeters”. Meter A was a 6” nominal bore Danfoss Sonoflo 3100 with a 4 path dual-cross mid-radius configuration. It was supplied with parameter logging software that enabled the path velocities to be recorded. Figure 2 shows the path configuration.

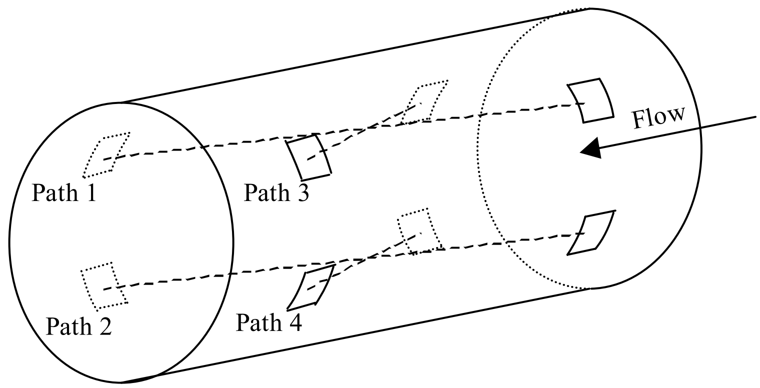

Figure 2 Path Configuration of Meter A

Meters B and C were supplied by Endress and Hauser, and Ultraflux respectively, and are both clamp-on meters with dual path capability. Both meters were clamped to individual 6” NB sch 40 pipe spools. Both were configured in a dual diametric configuration each path employing a single reflection. The path configuration is shown in Figure 3.

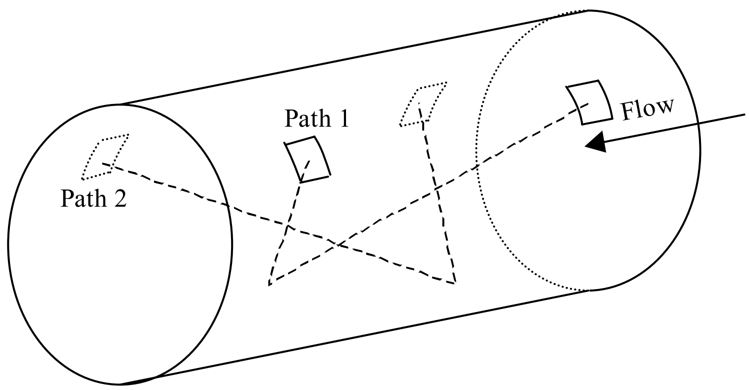

Figure 3 Path Configuration of Meters B and C

EXPERIMENTAL TEST METHOD

The installation effect tests reported here were conducted in the oil flow measurement National standard facility at NEL. The oil used was a lubricant oil with a viscosity of approximately 21 cSt at the test temperature of 20 degrees Celsius. The triple bend installation was installed in the test line upstream of the test meters. Figure 4 shows the layout of the tests. The test meters performance was measured by the master meter calibration method using a sliding vane positive displacement meter. Pulses were collected simultaneously from the test meter and reference PD meter for a given test interval. The expanded uncertainty (K=2) in the measurement of the quantity of fluid passed through the meter is ±0.08% for the master meter method.

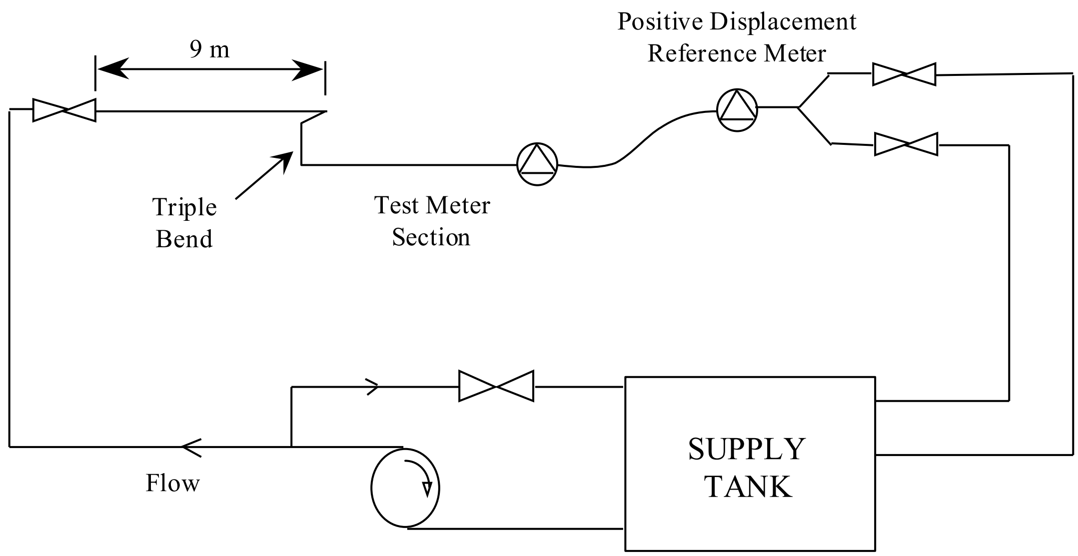

Figure 4 Diagram of Test Setup.

In addition to the triple bend installation tests, base line tests were performed on all the test meters. All meters had a minimum of 9metres (60 Diameters) upstream straight length in the baseline tests. The installation effect results shown in this paper are deviations from the baseline result at the same test velocity.

The individual path velocities were recorded on Meter A. The logging software recorded instantaneous velocity measurements at a rate of approximately one hertz for the duration of the test run. The velocity measurements for each path were averaged to determine the individual path velocities for each test run.

Figure 5 Triple Bend Test section

Figure 5 shows the triple bend and the test section. All test section pipework is 6" nominal bore sch 40. All the test section pipe spools were flanged, during the manufacture of the spools all weld burs were removed from the internal pipe surface. This ensured that the pipe conduit matched the CFD model as closely as possible. The triple bend comprised of three 90 degree long radius bends each with weld neck flanges at both ends. A set of pipe spools were fabricated which allowed the location of the test meters with reference to the triple bend to be adjusted by as little as one diameter (150mm).

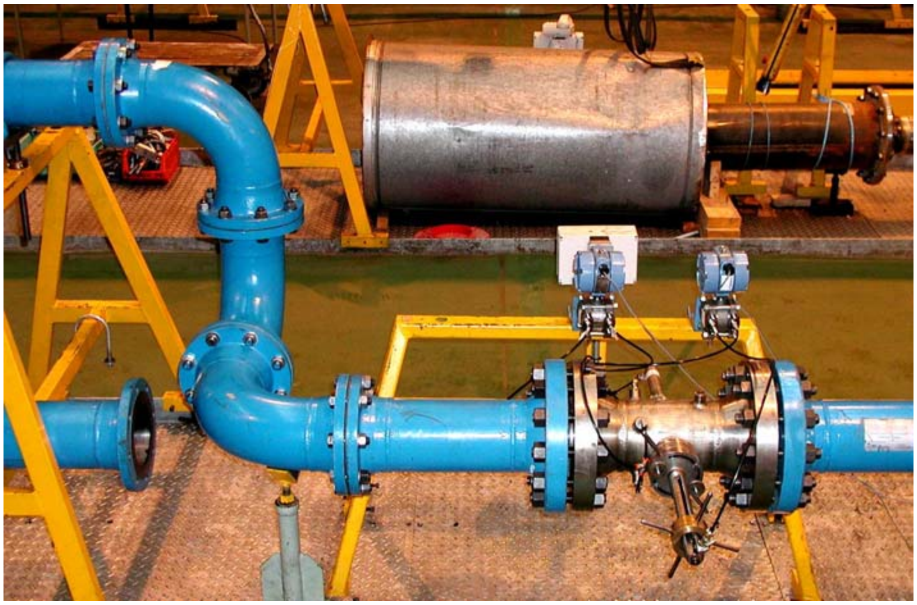

Figure 6 Pitot Tube Assembly and Triple Bend

The flow profile in the test section was measured using a traversing pitot tube. This measured both the swirl angle and the axial flow velocity at a range of points across the pipe diameter.

INSTALLATION EFFECT ON A DUAL-CROSS MID-RADIUS USM

Figure 7 shows the installation effect of the triple bend on meter A at 3 and 4 m/s. It clearly shows the installation effect fluctuating as the downstream distance is increased. The maximum deviation is just over 1.2%. This deviation is significant as the baseline test found the linearity of this meter to be 0.26% at velocities greater than 1 m/s. The installation effects at 3m/s and 4m/s are very similar, with the amplitude of oscillation appearing to reduce slightly at the higher flow rate.

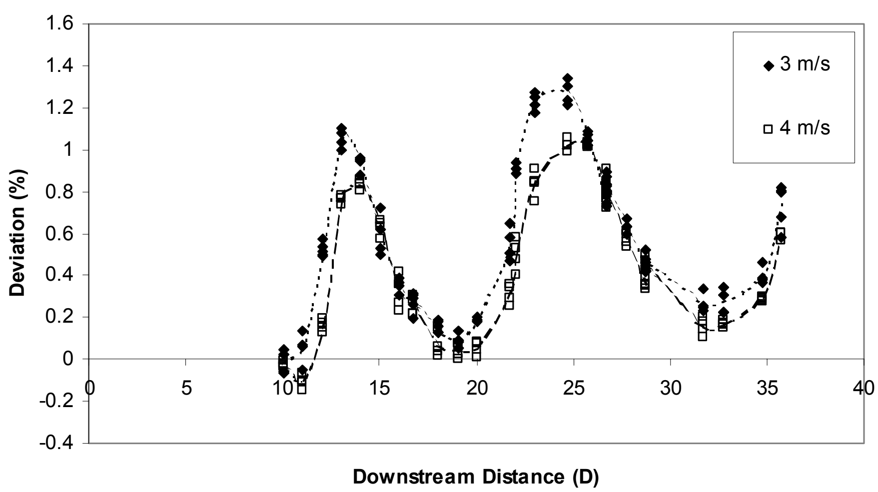

Figure 7 Installation Effect on Meter A (4 path Dual-cross Mid-radius)

We can gain an understanding of why the effect fluctuates by considering the individual path velocities. Figure 8 shows the individual path velocities normalised against the reference PD meter.

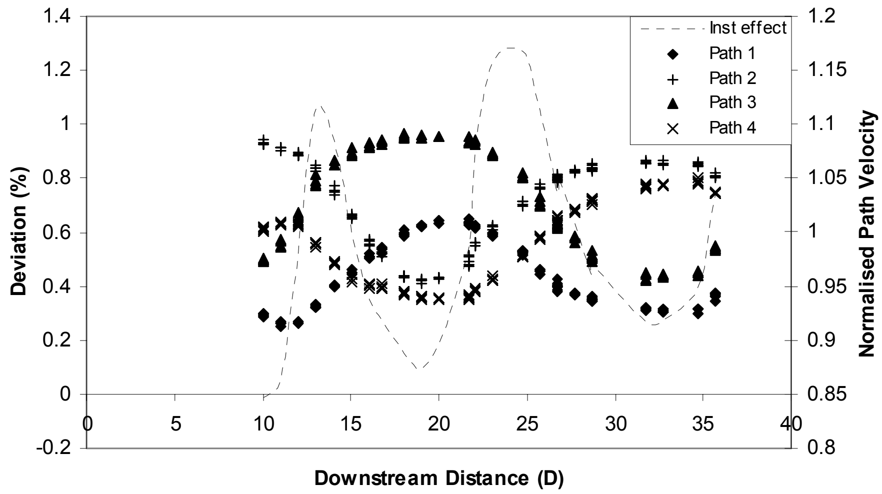

Figure 8 Normalised Path Velocities of Meter A

The path velocities oscillate as the distance from the triple bend is increased. They oscillate in two distinct "in phase" pairs, which correspond to the upper and lower path pairs. The pairs oscillate 180° out of phase with each other. The results of the paths in each pair are offset from each other by an amount that varies with downstream distance. This behaviour is compatible with a rotating distorted axial velocity flow regime i.e. bulk swirl. The following explains the results in terms of a bulk swirl flow regime.

Considering the axial velocities only, Figure 9 applies a theoretical bulk swirl flow onto a dual-cross mid-radius path design. Consider at point 1 the upper paths traverse the high axial velocity region and the lower paths traverse the low velocity region. The upper paths will measure a higher velocity than the lower paths. At point 2 both paths intersect the high and low axial velocity regions hence the path velocities are equal. And at point 3 the high and low regions are reversed hence so are the path velocities. Hence it is the axial flows of the bulk swirl that generate the path velocity oscillations.

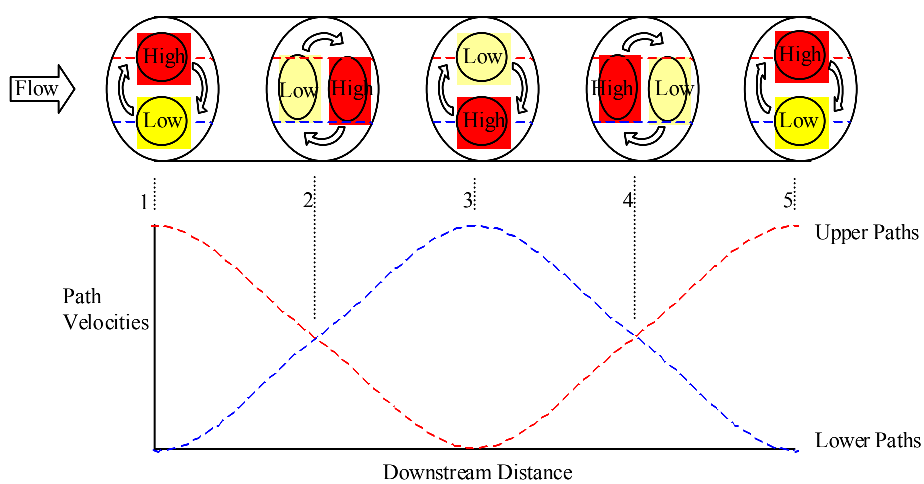

Figure 9 "Effect of Axial velocity profile"

The offset between the path pairs can be explained by the non-axial flows. Figure 10 shows how the non-axial flows interact with the lower ultrasonic paths of meter A. Any flow vector can be described in terms of its x, y and z components. In Figure 10 the axial flow is represented by the 'x' component with the non-axial flows represented by the 'y' and 'z' components. The ‘z’ component can be ignored since it is not on the plane of the lower paths. Therefore when discussing non-axial velocities we are really referring to the ‘y’ component. It should be noted that the ‘z’ component cannot be ignored when considering ultrasonic path deflection and propagation issues.

Consider the orientation of path 2 in Figure 10. Moving downstream path 2 crosses the flow from left to right, in the same direction as non-axial flow i.e. the ‘y’ component. This has the effect of increasing the measured path velocity. On path 4 the opposite occurs and the path velocity is reduced, resulting in an offset between the paths in that plane. A more detailed description of this effect is given in Reference 2.

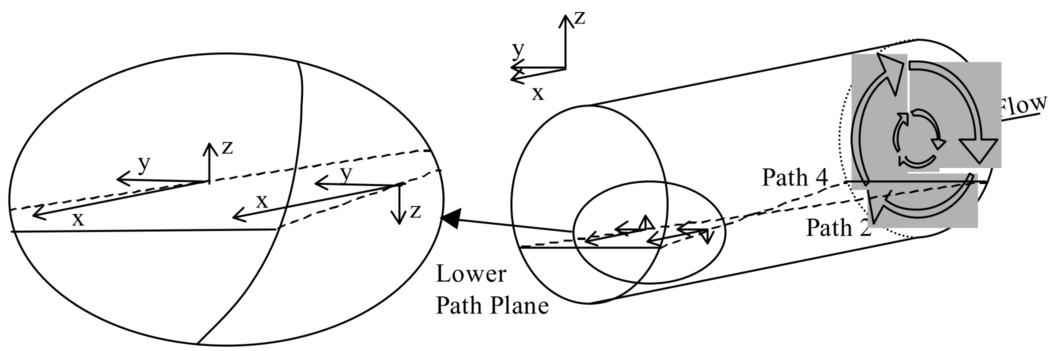

Figure 10 Effect of Non-Axial velocity profile

The offset in the lower paths (2,4) varies quite significantly as the downstream distance is increased. It is considered likely that this variation is due to the movement of the central axis of the bulk swirl. Consider Figure 11, when the bulk swirl axis moves towards the plane of the lower paths the non-axial velocity vector intercept the lower plane at almost 90°. Hence the ‘y’ velocity component is reduced while the ‘z’ component increases. This change in velocity components can be seen when the magnified sections of Figures 10 and 11 are compared. Since it is the ‘y‘ velocity component that affects path velocity then this change in the in-plane non-axial component is responsible for the variation in the offset.

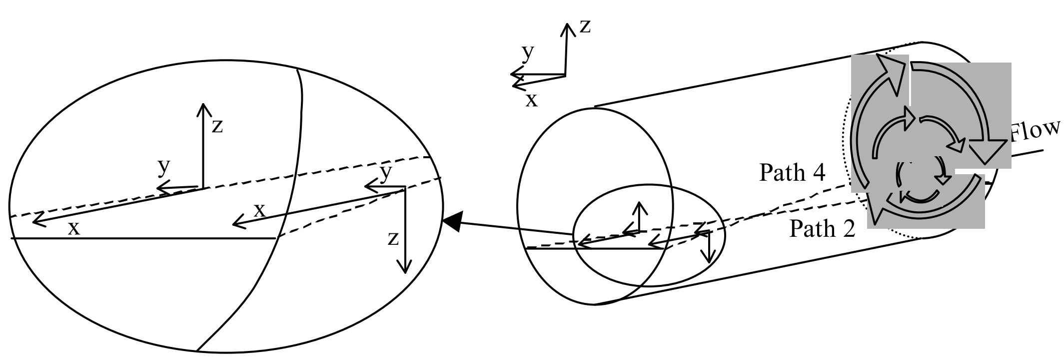

Figure 11 Effect of movement of axis of bulk swirl

Figure 12 shows how the movement of the axis of rotation can cause the change in the offset of the lower paths.

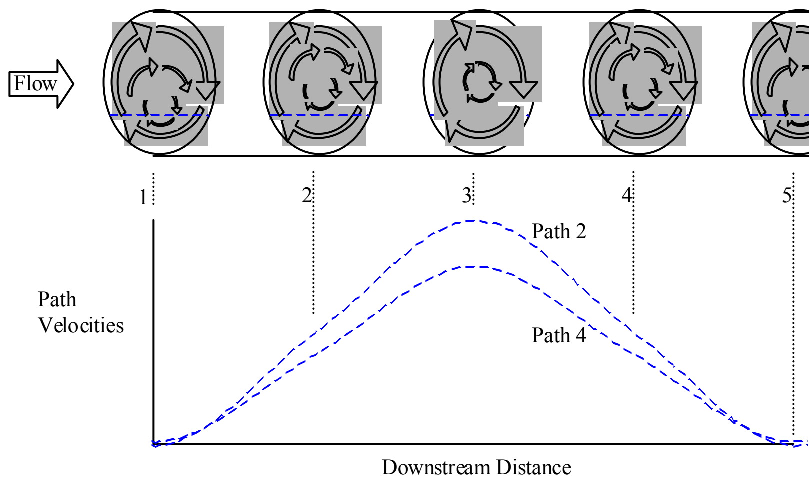

Figure 12 Overall Effect of movement of axis of bulk swirl

This indicates that the distorted axial and non-axial velocities present in the bulk swirl flow regime affect each path velocity. The effect of which is individual to each path depending on how the path interacts with the flow regime. This interaction is entirely dependent on the location and orientation of that path within the flow tube. Since the meter output is a combination of the individual path velocities, it is therefore the combination of these interactions that results in the observed oscillation in the meter performance.

INSTALLATION EFFECT ON ALTERNATIVE MID-RADIUS DESIGNS

Having obtained path velocity data for each path of the dual-cross mid-radius meter. It is possible to evaluate other path designs from the data. Figure 14 shows the results of a reconstruction of the full dual-cross meter compared against the meters pulse output. It can be seen that the reconstructed and pulse outputs match closely.

Other path designs were simulated using this experimental data, Figure 13 shows the simulated path arrangements. The two designs are essentially the same, meter type A1 being the inverted version of meter type A2. The design is a commonly used two path dual mid-radius type.

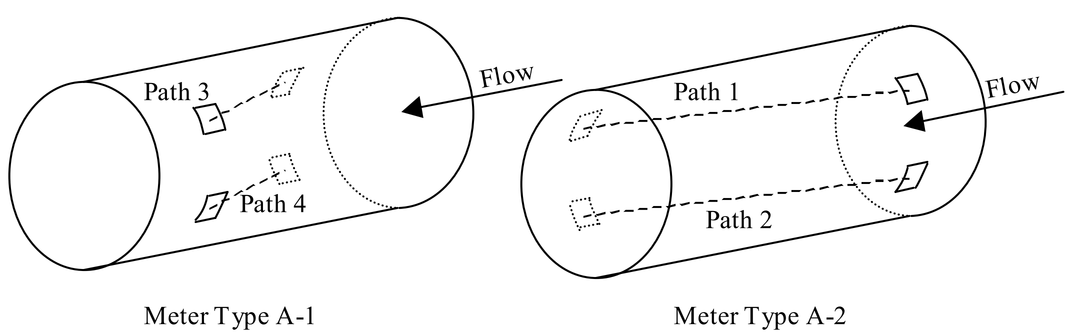

Figure 13 Meter Designs reconstructed from path velocity data

The installation effects on the two path designs are as expected, larger than on the four path design. These results clearly show the sensitivity of meter performance to the specific path design. Although both designs are essentially the same, the installation effects vary by as much as 3.7%.

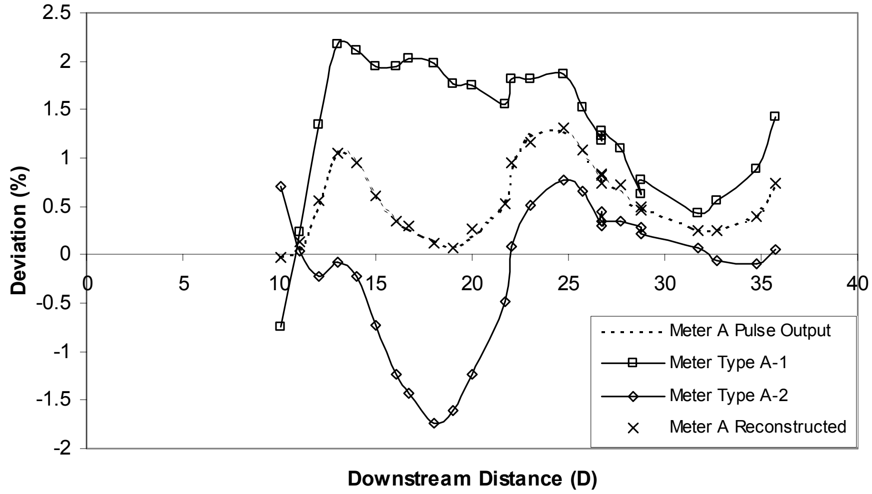

Figure 14 Reconstructed meter results

INSTALLATION EFFECT ON CLAMP-ON USM'S

Figure 15 shows the installation effects on the clamp-on ultrasonic meters when in single 'V' path mode with a flow rate of 4m/s. Both meters installation effects are very similar, there only being at most about a 1% difference between them. This is most likely due to the meters employing slightly different profile correction factors. The installation effect characteristic is comprised of two parts, an offset that diminishes as the downstream distance increases and a superimposed oscillation. The oscillation amplitude increases, and it period lengthens as the downstream distance increases. Between 10 and 15 diameters the period is approximately 8-9 diameters.

The oscillation seems to be caused by the rotation of the distorted axial velocity profile, in a process similar to that seen in the individual paths of the dual-cross mid-radius meter.

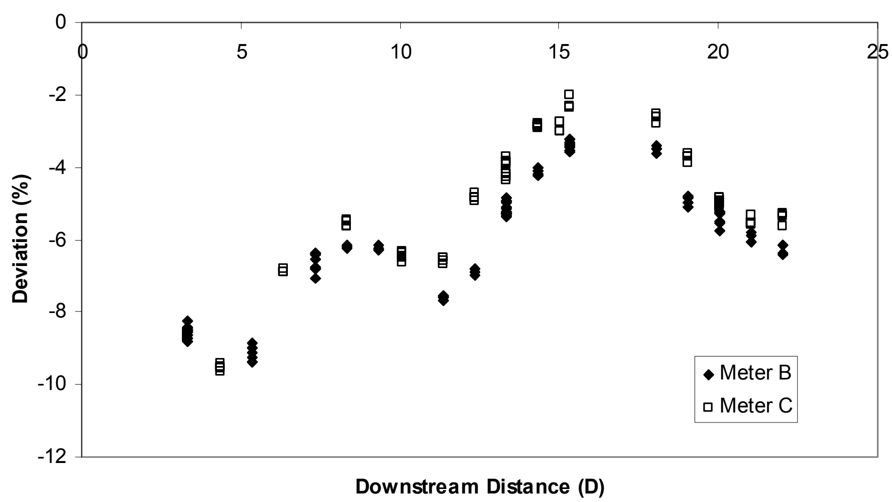

Figure 15 Installation Effect on Single V Path Clamp-on Meters

Figure 16 shows the installation effect on meter B when setup in the Dual "V" path configuration, the effect on the single path design is also shown for comparison. The dual path installation effect also consists of a diminishing offset and an oscillation. The offset in both meter designs are very similar. They are both negative and diminish at the same rate over distance. This suggests that the offset is caused by a general flattening of the flow profile.

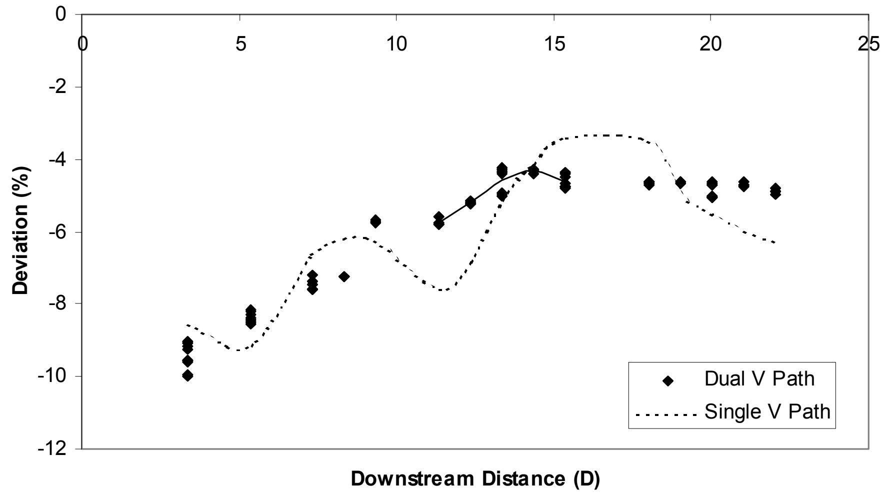

Figure 16 Installation Effect on Meter B (Clamp-on)

The oscillation of the dual "V" path configuration is difficult to distinguish as it seems to have a period similar to the spacing of the test points. Between 11 and 16 diameters downstream where the test spacing was 1 diameter the effect shows an oscillation with a possible period of approximately 4 diameters. The oscillation is more difficult to identify closer to the bend because the test spacing was greater. It also seems to have a reduced amplitude compared to the single path. The oscillation does not seem to extend into the 18 to 23 diameter region.

This analysis of the single path and dual path characteristics has shown that adding reflected diametric paths to the measurement reduces the amplitude of the oscillations but does not affect the overall meter offset.

DIAGNOSTIC POSSIBILITIES OF PATH VELOCITY DATA

One of the major advantages of ultrasonic meters is the diagnostic data that is available for analysis. During these tests the path velocities were recorded and have been assessed for their diagnostic potential.

Dual-cross Mid-radius Meter Diagnostics

Meter A with four ultrasonic paths has the greatest potential for providing information via diagnostic parameters as it has four independent velocity measurements. Four sets of velocity data allow several methods to be employed to analyse the flow and attempt to predict meter performance.

Having two paths in cross formation on a mid-radius plane, allows the magnitude of non-axial flow in each plane to be quantified.

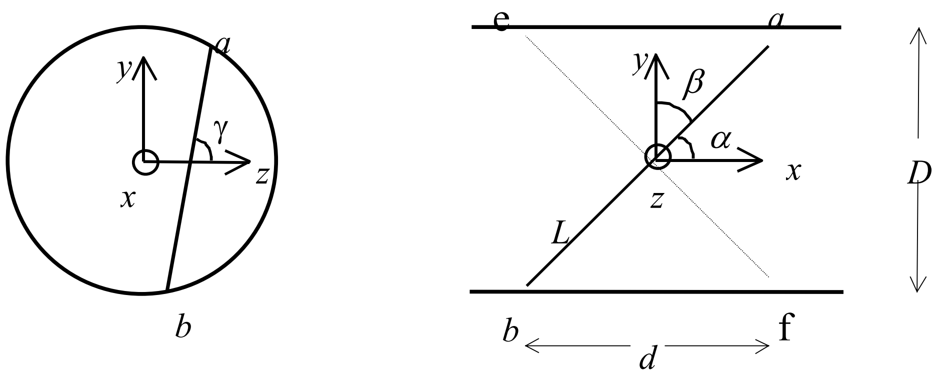

Figure 17 Ray Geometry Transit Time Meter

Consider Figure 17, the path velocity on path a-b ($\overline{v}_{ab}$) is:

$$\overline{v}_{ab} = \overline{v}_x + \overline{v}_y \frac{D}{d}$$

Similarly, the path velocity on path e-f is:

$$\overline{v}_{ef} = \overline{v}_x - \overline{v}_y \frac{D}{d}$$

Subtracting one velocity from another gives:

$$\overline{v}_{ab} - \overline{v}_{ef} = 2\overline{v}_y \frac{D}{d}$$

Hence the averaged non-axial or 'swirl' velocity on the plane is:

$$\overline{v}_y = \frac{d}{D}\left(\frac{\overline{v}_{ab} - \overline{v}_{ef}}{2}\right)$$

A reasonable diagnostic parameter might be to sum the magnitudes of the non-axial flows in the upper and lower planes to give a total non-axial or 'swirl' indicator (Swirl Diagnostic). That is:

$$\text{Swirl Diagnostic} = \text{Abs}\left(\overline{v}_{y(\text{Upper})}\right) + \text{Abs}\left(\overline{v}_{y(\text{Lower})}\right)$$

A high swirl diagnostic would relate to a higher degree of swirl hence a greater installation error. The swirl diagnostic has been plotted in Figure 18 with the meter's installation effect superimposed. It shows a degree of agreement with the swirl diagnostic maxima occurring at the peaks of the installation error. However it does not fully correlate, further parameters are required to make this parameter a truly useful diagnostic tool.

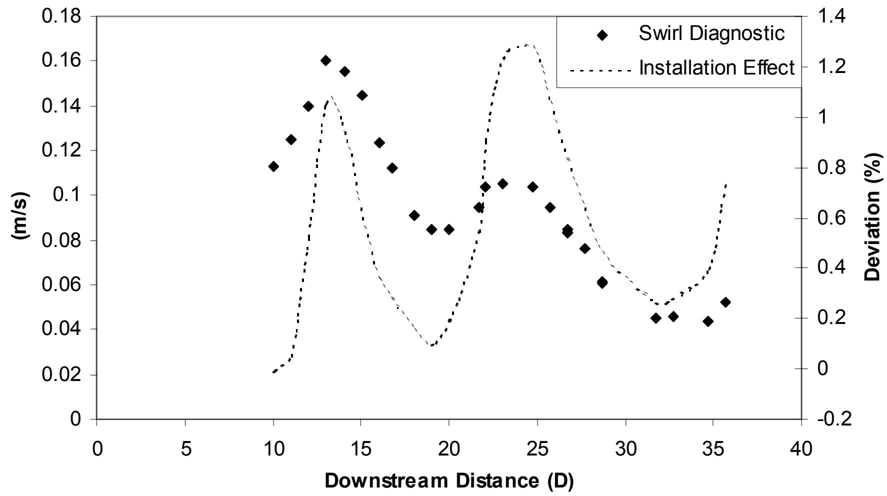

Figure 18 Swirl Diagnostic Indicator

Alternatively the axial flow in each of the upper and lower planes can be quantified, by averaging the cross path velocities in each plane. Consider again Figure 17, adding the path velocities gives:

$$\overline{v}_{ab} + \overline{v}_{ef} = 2\overline{v}_x$$

Hence the averaged axial velocity in the plane is:

$$\overline{v}_x = \frac{\overline{v}_{ab} + \overline{v}_{ef}}{2}$$

A reasonable diagnostic might be to take the magnitude of the difference between the axial velocities (Axial Diagnostic). That is:

$$\text{Axial Diagnostic} = \text{Abs}\left(\overline{v}_{x(\text{Upper})} - \overline{v}_{x(\text{Lower})}\right)$$

The greater the value of the axial diagnostic parameter the greater the apparent distortion in the flow profile hence we might expect a larger installation effect. Figure 19 shows the axial diagnostic with the installation effect superimposed. This diagnostic behaves exactly counter to what was expected, it shows that in this flow regime the meter operates best when the axial velocities are unequal. This result is counter intuitive and will not apply to all flow regimes.

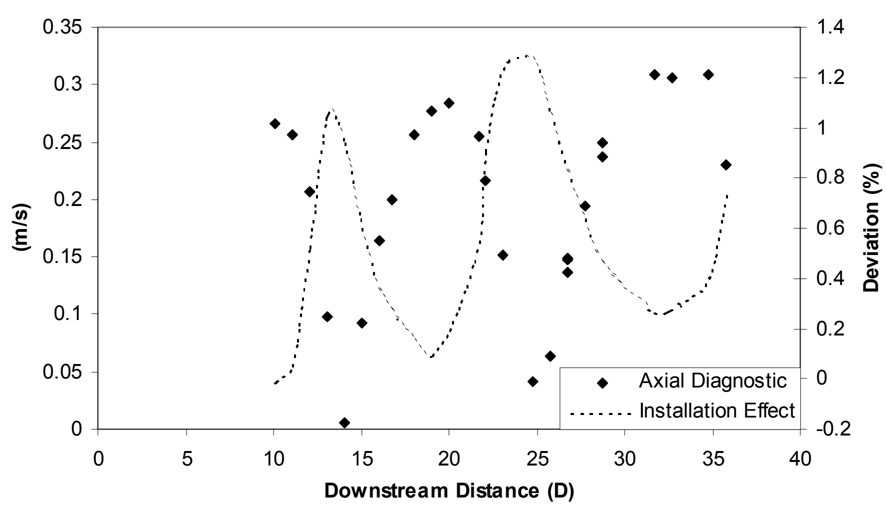

Figure 19 Axial Velocity Diagnostic Indicator

These two path velocity diagnostic parameters highlight the need for further diagnostic data to determine meter performance. The path velocity data available in the dual-cross mid-radius design does not provide sufficient information on the flow profile to predict meter performance in this test case.

Dual "V" Path Clamp-on Diagnostics

The clamp-on meters used in the project can operate in single or dual path mode. Obviously there is not much that can be done with a single path. However in the case of the two path meter it is possible that a measure of the meter's performance could be inferred from how closely the path velocities agree.

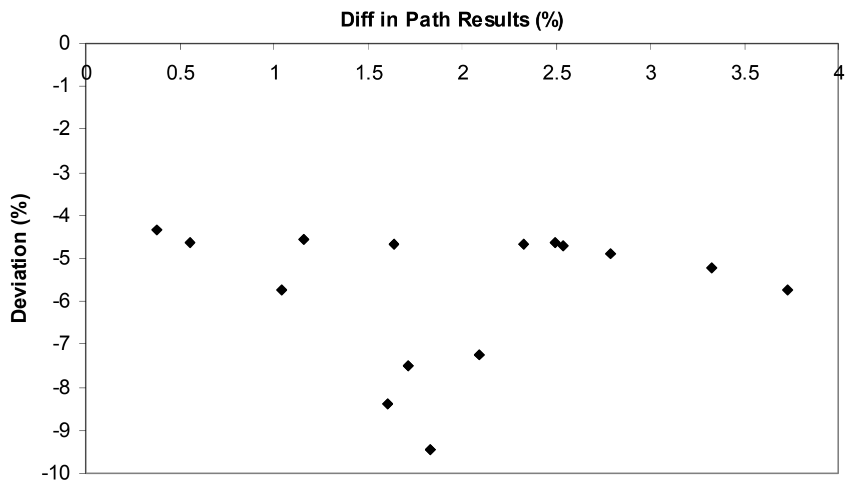

Figure 20 Dual "V"Path Clamp-on Difference in Path Velocity as Diagnostic

Figure 20 shows the percentage difference between the paths of a dual "V" path meter against its installation effect. As can be seen there is no correlation. The difference in the path velocities gives no indication of meter performance.

CFD MODELLING OF INSTALLATION EFFECT

This section of the paper presents the results of the CFD modelling of the laboratory experiments.

CFD Simulation Method

All CFD simulations used the Fluent 6.0 code. The QUICK discretisation scheme was used to minimise numerical errors. Turbulence effects were accounted for by using the Reynolds Stress turbulence model (RSM).

The solution process involved introducing a fully developed flow profile into a model representing the triple bend. The mesh for the triple bend is shown in Figure 21. The disturbed outlet profile calculated in this simulation was then used to define the inlet conditions of second simulation which modelled the flow through the test section in which the ultrasonic flowmeters were installed.

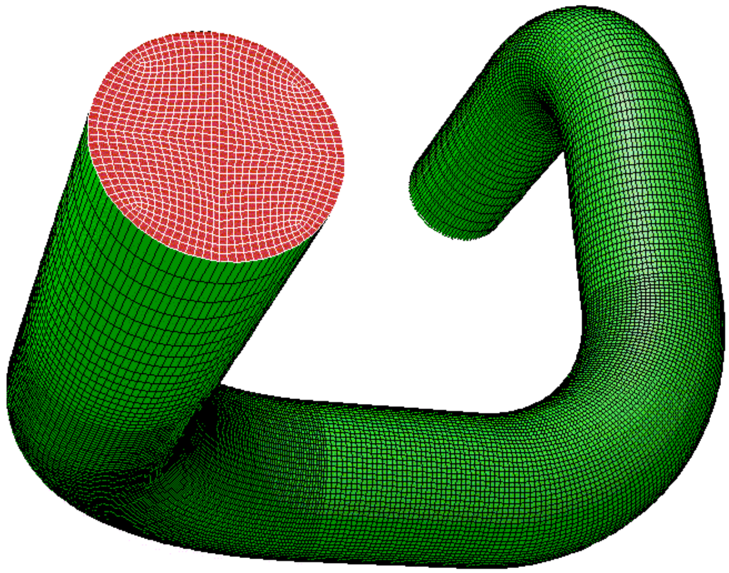

Figure 21 Computational mesh used for simulating the flow through a triple out-of-plane bend

In the virtual flowmeter lines were defined across the bore of the pipe which represented the ultrasonic paths. The path velocities were calculated thus:

$$\bar{v}_{path} = \frac{1}{L\cos\theta}\int_{-L/2}^{L/2} v(l)dl$$

Path velocities were then combined to calculate the volumetric flow rate in the manner that is used in the real flowmeters.

Comparison of Test Measurements and CFD Predictions

Figures 22 and 23 show velocity and swirl profiles measured downstream of the bend by means of a Pitot tube traverse. Figure 22 shows that the CFD correctly predicts the magnitude of swirl and the fact that the centre of swirl is offset from the axis. Figure 23 shows that the measured profile is slightly flatter than the predicted profile. The CFD results also show a double maximum (at r/R of about ±0.7), which is more exaggerated than in the test data.

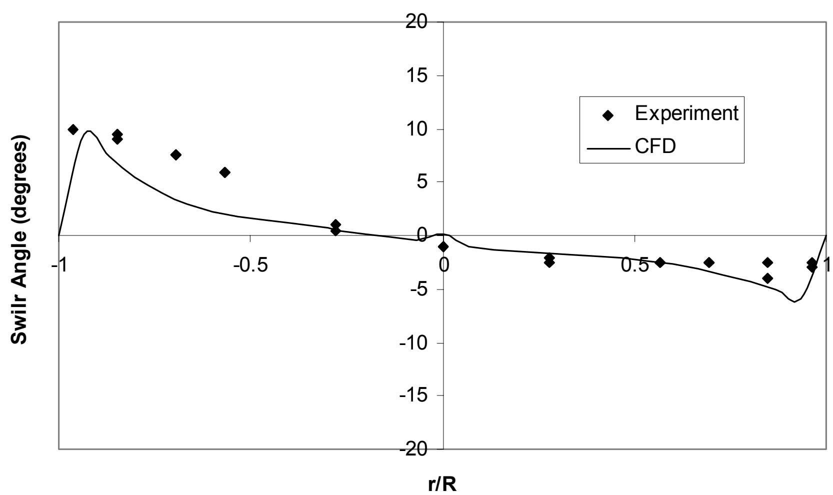

Figure 22 Measured and predicted swirl angle 20 diameters downstream of the double bend

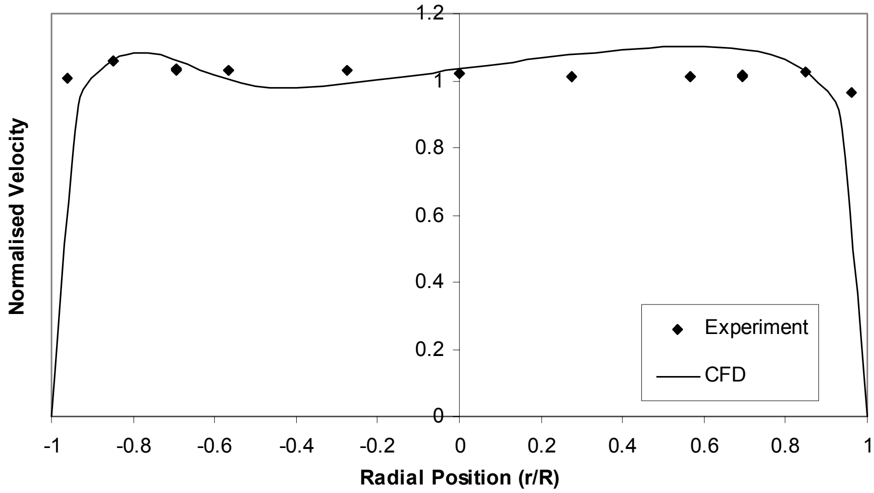

Figure 23 Measured and predicted axial velocity profile 20 diameters downstream of the double bend

Figure 24 shows the predicted behaviour of the flow downstream of the triple bend. The triple bends generate a swirling flow. The centre of swirl is offset from the centre of the pipe and it spirals down the pipe as the distance from the triple bend increases. Flow leaving the last bend is thrown to one side of the pipe generating a high velocity region at the top left hand side of the pipe at 0D. The swirling flow causes this high velocity region to spiral down the pipe. This behaviour is similar to that illustrated in Figures 9 and 12.

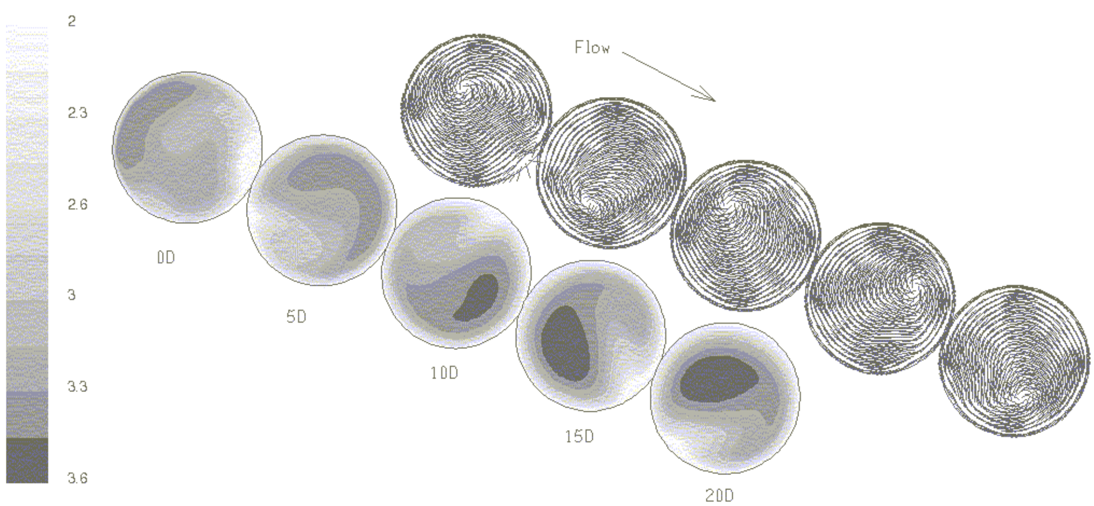

Figure 24 Predicted contours of axial velocity and transverse vectors at different distances downstream of the triple bend

Figure 25 shows the predicted and measured error characteristics of the clamp-on meters downstream of the triple bend. The CFD correctly predicts the trend and magnitude of the error and the fluctuating behaviour of the error characteristic is reproduced. The amplitude of the fluctuations is also in good agreement. As discussed previously it is dificult to determine the fluctuation frequency from the experimental data. However the CFD agrees with the most likely value as taken from the experimental data of a period of approximately 4 to 5 diameters.

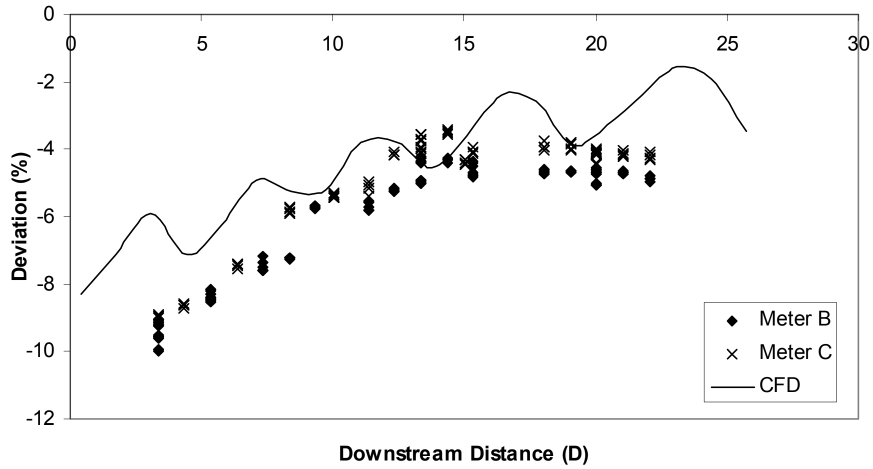

Figure 25 Predicted and measured error characteristic of the dual diametric clamp-on meters

Figure 26 compares the predicted and measured error characteristic of the four-path meter. Again the CFD correctly predicts the fluctuating nature of the error characteristic, but exaggerates its frequency and amplitude. The mean predicted error in the 10 to 35 diameter range is –1% compared to a measured value of +0.4%. This difference in absolute value is caused by the fact that the predicted axial velocity profile is more rounded than the actual profile.

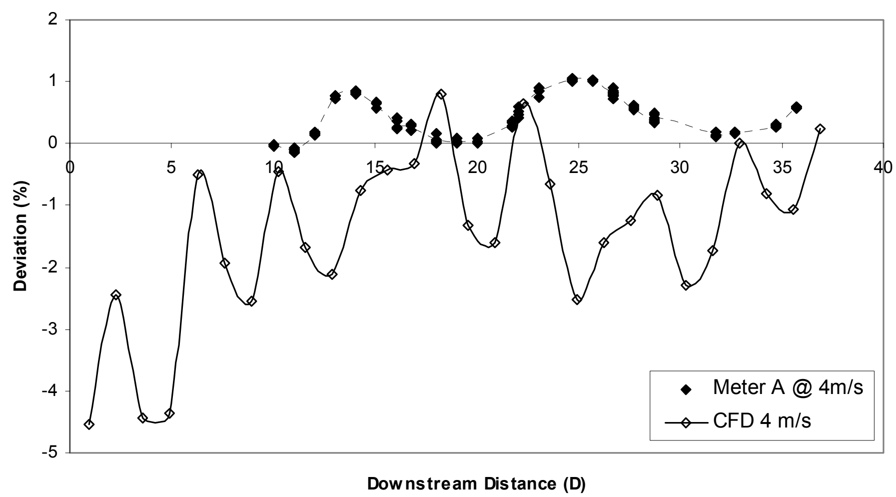

Figure 26 Predicted and measured error characteristic of the four path dual mid-radius meter

Examination of the individual path velocities (Figure 27) shows that the CFD predicts a low frequency high amplitude oscillation with a superimposed high frequency low amplitude fluctuation. The high amplitude oscillations agree reasonably well with the measured path velocities. The higher frequency oscillations are not seen in reality and they are the source of the exaggerated oscillations seen in the predicted error characteristic (Figure 26).

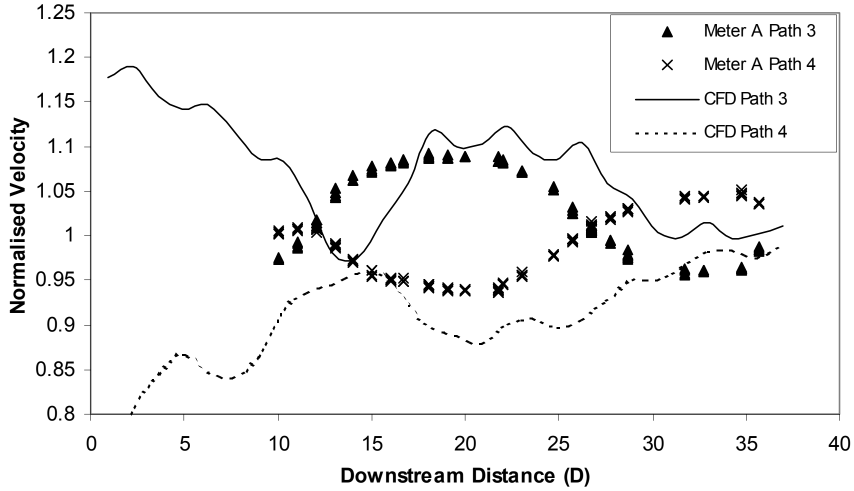

Figure 27 Predicted and measured error path velocities of two of the paths of the four-path dual mid-radius meter

CONCLUSIONS

The error of ultrasonic flowmeters installed downstream of triple bends has been shown to vary in a complex manner. In-depth analysis of test data has shown that:

- All meters tested were affected to a significant amount.
- Increasing the number of multiple mid-radius paths results in a reduction of installation effects.
- Increasing the number of multiple diametric paths does not necessarily reduce installation effects.
- Installation effects are highly sensitive to path design.
- Installation effects are still significant at the greatest downstream distances tested (35 diameters in the case of meter A). The distance downstream at which the installation effect is no longer significant has not been established.
- The oscillatory nature of the effect can result in significant variations within short changes of downstream distance.
- The velocity data from a dual-cross mid-radius meter does not contain sufficient information on the flow regime to enable prediction of the installation effect.
- In the case of multi path diametric meters performance cannot be inferred from comparison of path velocities.

In addition to this, CFD flow simulation methods have been used to study installation effects in ultrasonic flowmeters. Based on the findings of this work and similar work performed at NEL the following conclusions can be made:

- It is reasonable to use CFD methods to:
  - identify problems in ultrasonic flow metering installations
  - gain an understanding of the cause of these problems
  - assess the magnitude of installation errors
  - assess the effectiveness of different remedial measures
  - extrapolate laboratory results for application to field problems

The CFD methods outlined in this paper consistently reproduce the flow behaviour seen in the laboratory and in the field. In most cases a good quantitative match between predictions and measurements has been achieved. However, for some installations, although trends are well represented, there can be a significant difference between measured and calculated meter errors. It is unlikely therefore that CFD methods could be used solely to recalculate meter factors in applications. The results can be considered suitably accurate for use in evaluation of measurement uncertainty and assessment of meter station design.

ACKNOWLEDGEMENTS

The work described in this paper was carried out as part of the Flow Programme 1999-2002 under the sponsorship of the DTI's National Measurement System Directorate. The authors would also like to thank The Danfoss Group, Ultraflux and Endress and Hauser for the loan of their meters.

REFERENCES

1. BARTON, N. A.. Velocity distribution effects on ultrasonic flowmeters. Part 2 – Determination by computational and experimental methods. 1996-99 Flow Programme Report, NEL Report No 358/99, 20 September 1999.

2. COULL, C. J. In-service Performance of Ultrasonic Flowmeters – Initiation Phase Report. 1999-2002 Flow Programme Report, NEL Report No 144/2000, 6 July 2001.